Technical paper

TH STZ1 01

ADAPTIVE WINDOWED DEGHOSTING - APPLICATIONS TO FAZ ACQUISITION

Authors – Z. Zhang* (TGS), Z. Wu (TGS), B. Wang (TGS) & J. Ji (TGS)

Summary

The success of de-ghosting depends on accurate estimation of the ghost delay time, explicitly,or implicitly. We propose the use of the L1 norm in searching for the ghost delay time, afterdividing data into overlapping windows. The adaptive de-ghosting method has been testedusing both synthetic data and field data, including wide azimuth (WAZ) and full azimuth (FAZ)data. Its adaptive nature makes it applicable for data with 3D effects, and robust to uncertaintiesin receiver depth and water velocity.

Introduction

In marine acquisition, up-going waves are reflected from the water surface, causing both source and receiver side ghost effects. Ghosts closely follow primaries in seismic data with opposite polarity, interfere with the primaries, and introduce ghost notches in the amplitude spectrum. Attenuating the ghost effect broadens the available frequency band and helps to obtain high resolution images. Research to separate ghost and primary started decades ago (Jovanovich et al., 1983). It has attracted a great deal of attention recently as substantial progress has been made in both acquisition and processing stages.

The ghost notch depends on the streamer depth directly; therefore receiver depth variation contributes further to the receiver notch diversity. The slant cable (Soubaras, 2012) design and dual depth streamer design (Posthumus, 1993) are typical examples in this category. The multisensor design, on the other hand, recovers lost information in the hydrophone with signals from geophones (Carlson et al., 2007). The processing-based deghosting algorithms for conventional data acquisition also receive great interest because of the obvious benefit from deghosting and wide availability of legacy data (Zhou et al., 2012; Masoomazadeh et al., 2013; Telling et al., 2014; Wang et al., 2014; King, 2015). An accurate estimation of the ghost delay time, the time gap between the primary and ghost, is critical for these algorithms. Most of these algorithms work in the frequency domain and use a tau-p transform to decompose the wave field into local plane waves.

Because of the sparse sampling in the crossline direction, 2D tau-p transforms are widely utilized for deghosting in practice. However, the 2D transform only provides slowness along the streamer direction, *px*, which is not sufficient to determine the ghost delay time. 3D effects, such as reflections from off-plane events, result in time-variant ghost delay times even in the same *px* plane. Wang proposed an inversion-based 3D deghosting method (Wang et al., 2014) using a sparseness constraint in the tau-p domain. In this abstract, we propose an alternative algorithm to deghost wide azimuth (WAZ) and full azimuth (FAZ) data using a 2D tau-p transform. The core of our algorithm is an adaptive ghost delay-time search engine, which we use to build a time-variant deghosting procedure. Both synthetic and field data tests have shown the algorithm to be very stable and robust. We use WAZ and FAZ acquisitions in our examples because they are more challenging than narrow azimuth (NAZ) data. Firstly, the slowness in the crossline direction (*py*) is mostly nonzero, which invalidates any 2D assumption. Secondly, guns are positioned to the side of some cables with substantial distance. Offset change is very fine when the azimuth approaches 90 degrees. Last but not least, the source signature is directional. Sometimes, the source adds an inherent notch in the frequency spectrum close to the ghost notch and makes QC and deghosting more difficult.

Method for adaptive deghosting using small windows

The sea surface is generally not smooth, and a rough surface causes scattering. The reflection coefficient at the water-air interface is actually a function of frequency, emerging angles, and wave conditions (Jovanovich et al., 1983). Similar effects could also be observed after discrete tau-p transforms, since energy may leak from one slowness value to its neighborhood. In this abstract, we assume a Gaussian-type function for the reflection coefficient, as

$$r(f) = \mathrm{e} - \frac{1}{\sigma 2} f^2 \ .$$

The positive number σ controls how fast the reflection coefficient changes with frequency and is related to the sea-wave height. We perform deghosting in the frequency domain with the ghost operator given by

$$G(f) = 1 - \ r(f) e^{-i2\pi f \Delta_r},$$

where Δ*r* is the true ghost delay time. When σ becomes very large, (*f*) gets close to 1, and the operator converges to the calm water surface case,

$$G(f) = 1 - \ e^{-i2\pi f \Delta_r}.$$

We use the inverse of the ghost operator as the deghosting operator in the frequency domain,

$$F(f) = \frac{1}{1 - r(f) e^{-i2\pi f \Delta_a}}$$

Here Δα is the actual delay time used. The obtained deghosted data, denoted as (*f*), can then be written as

$$P_{dg}(f) = \frac{1-r(f)e^{-i2\pi f\Delta_r}}{1-r(f)e^{-i2\pi f\Delta_a}}\,P(f)$$

where *P*(*f*) is the true primary without ghost.

In practice, small windows of seismic normally do not have enough data to support statistical measures like autocorrelation, amplitude spectrum, or phase spectrum, under influence from noise and geology. When a data set is small, the L1 norm or L2 norm minimization behaves better since correctly deghosted data tends to be clean and have less energy. Kurtosis maximization has also been reported in the search of ghost delay time (Grion et al., 2015). To fairly compare the L1 norm, L2 norm, and kurtosis, we normalize them using the ghost-free primary. In Figure 1, the three curves shown are, respectively,

$$J_1 = \frac{|P(t)|_{L1}}{|P_{dg}(t)|_{L1}}$$

for L1 norm,

$$J_2 = \frac{|P(t)|_{L2}}{|P_{dg}(t)|_{L2}}$$

for L2 norm,

$$J_k = \frac{k\,(P_{dg}(t))}{k\,(P(t))}$$

for kurtosis. The kurtosis is a statistical measure defined as, where η is the mean of Δ. We use a 20 ms ghost delay time and Δ=240 Hz in the example. The input data have multiple events and are put in a 2 s time window. We scan Δ_α from 6 ms to 40 ms and calculate the three functions. It is interesting to notice that the L1 norm almost overlaps with the kurtosis when noise does not exist, and it is even sharper near the right answer. All three functions successfully locate the right ghost delay time. In the next test, we add Gaussian white noise in the data. The amplitude of the noise is controlled so that the signal-to-noise ratio is 20 dB. Again, all three functions located the ghost delay time with reasonable accuracy. Near 20 ms, the L1 norm is almost as sharp as the kurtosis, but is more flattened when Δ_r is away from 20 ms. The situation is more complicated in field data. We use the L1 norm in our search since it is easy to calculate and it behaves more robustly than either the kurtosis or L2 norm in many field data tests. A global search is applied to make sure the search will not end in a local optimal value.

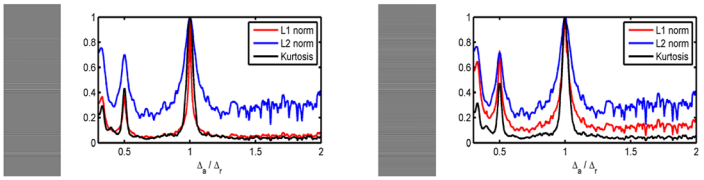

Figure 1 Comparison between the L1 norm, L2 norm, and kurtosis. a) Without noise. The left panel shows the input data, and the object functions are drawn in the right panel. b) With Gaussian white noise added in the background. All three functions successfully found the right ghost delay time in both cases.

A rough estimation of Δ_α mostly available in practice and the search range can be much smaller than is shown in Figure 1. This makes the searching even more robust. The parameter σ affects the shape of the objective function, but does not change the location of the minimum. We also take advantage of a high resolution tau-p transform and apply deghosting in the tau-p domain

Field data examples

The data used in our test is a FAZ data set from the Gulf of Mexico. The acquisition has a staggered configuration partially shown in Figure 2. The crossline distance between the gun and cable is about 2.4 km, causing serious 3D effects. When the azimuth is close to 90 degrees, the smallest offset change from one receiver to a neighbor receiver is about 0.03 m. We regularize the offset before the tau-p transform. Careful investigation is applied to make sure the input could be honestly recovered by an inverse transform without losing weak events or steep events. The source depth is fixed at 10 m and the cable is towed flat at 12 m.

Beginning with a shot gather, Figure 2 shows the comparison before and after deghosting on both source and receiver sides. Ghost energy is greatly attenuated everywhere. The high resolution tau-p transform separates the crossing events nicely and makes the adaptive deghosting successful, even for diffractions and crossing events. The input data has strong 3D effects, which can be shown by the spectrum of the water bottom, shown in the red box, and the first order multiple of the water bottom, shown in the green box. Though they share similar inline slowness values, their amplitude spectra indicate different ghost notches. The first nonzero ghost notch of the water bottom is near 83 Hz, while that of the multiple is about 67 Hz. This difference is taken into account by the adaptive algorithm.

Both are well deghosted, and achieve similar spectra after deghosting.

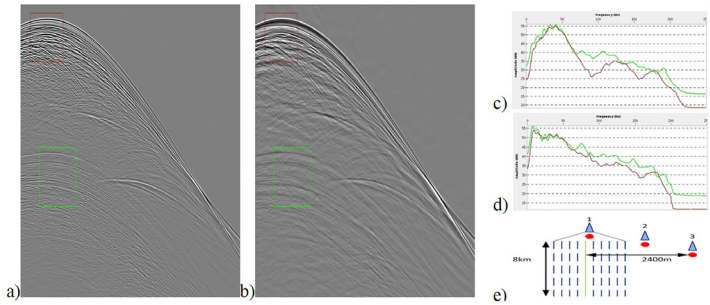

Figure 2 A shot gather before and after deghosting from a FAZ acquisition. a) Input data before deghosting; b) After both source and receiver deghosting; c) Input amplitude spectra of the region near water bottom (red box and red curve) and near first-order multiple of water bottom (green box and green curve); d) Amplitude spectra after deghosting; e) Gun-cable configuration. The acquisition utilizes 5 vessels. Only three are shown here because of limited space. The data used in this abstract is acquired using gun 3 and the cable in solid line.

Conclusions

WAZ and FAZ acquisitions have strong 3D effects and cause great difficulties for regular 2D tau-p deghosting. We propose the use of the L1 norm as a search criterion for the ghost delay time in small windows after a high resolution tau-p transform. The adaptive windowed deghosting algorithm has been successfully applied in many projects, including NAZ and WAZ data, and shallow and deep water data. Its adaptive nature makes it very flexible and not limited in the tau-p domain. Both receiver-side and source-side ghosts can be treated with the same strategy.

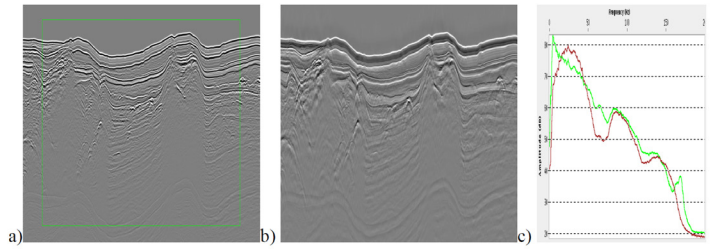

Figure 3 Stacked image before and after deghosting. a) Input data; b) After deghosting on both source and receiver sides; c) Amplitude spectrum from the region in the green box. Spectrum for the input data is show in red, while spectrum for the deghosted data is shown in green.

Acknowledgements

The authors are grateful to TGS for permission to include the Declaration data in this abstract. We also wish to thank Sampad Laha and Hassan Masoomzadeh for inspiring discussions, and Roy Camp and James Espinosa for preprocessing the data.

References

Carlson, D.A., Long, W., Tobti., H., Tenghamn, R., and Lunde, N. [2007] Increased resolution and penetration from a towed dual-sensor streamer, First Break, 25, 71-77 Grion, S., Telling, R., and Barnes, J. [2015], De-ghosting by kurtosis maximisation in practice, 85th Annual International Meeting, SEG, Expanded Abstracts, 4605-4609 Jovanovich, D.B., Sumner, R.D., and Akins-Easterlin, S.L. [1983] Ghosting and marine signature deconvolution, a prerequisite for detailed seismic interpretation, Geophysics, 48, 1468-1485.

King, S. and Poole, G. [2015] Hydrophone-only receiver de-ghosting using a variable see surface datum, 85th Annual International Meeting, SEG, Expanded Abstracts, 4610-4614 Masoomazadeh, H. and Woodburn, N. [2013] Broadband processing of conventional streamer data-optimized de-ghosting in the Tau-P domain, 75th EAGE Conference & Exhibition incorporating SPE EUROPEC, London, UK Posthumus, B. J. [1993] De-ghosting using a twin streamer configuration, Geophysical Prospecting, 41, 267, 267-286.

Soubaras, R. [2012] Pre-stack de-ghosting for variable-depth streamer data, 74th EAGE Conference & Exhibition incorporating SPE EUROPEC, Copenhagen, Denmark, I019 Telling, R., Riddalls, N., Azmi, A., Grion, S., and Williams, R. [2014] Broadband processing of west of Shetland data, First Break, 32, 97-103 Wang, P., Ray S., and Nimsaila K. [2014] 3D joint de-ghosting and crossline interpolation for marine single-component streamer data, 84th Annual International Meeting, SEG, Expanded Abstracts, 3594-3598.

Zhou, Z., Cvetkovic, M., Xu, B., and Fontana, P. [2012] Analysis of a broadband processing technology applicable to conventional streamer data, First Break, 30, 77-82.

About TGS

TGS is headquartered in Oslo, Norway, and publicly traded on the Oslo Stock Exchange. Our other main offices are in Calgary, Houston, London and Perth, and we have employees in cities around the globe. Our primary business is to provide geoscience data to energy companies worldwide. We offer extensive global libraries that include seismic data, magnetic and gravity data, multibeam and coring data, digital well logs, production data and directional surveys. Additionally, we offer advanced processing and imaging services, interpretation products and data integration solutions.

For more information, contact TGS at:

US
Tel: +1 713 860 2100

Email: sales@tgs.com

See the energy at **TGS.com**

TGS